

Health monitoring of pedestrian truss bridges using cone-shaped kernel distribution

Hamid Reza Ahmadi^{*1} and Diana Anvari^{2a}

¹Department of Civil Engineering, Faculty of Engineering, University of Maragheh, Maragheh 55181-83111, Iran

²Department of Civil Engineering, Bandar Abbas Branch, Islamic Azad University, Bandar Abbas, Iran

(Received March 31, 2018, Revised July 6, 2018, Accepted November 11, 2018)

Abstract. With increasing traffic volumes and rising vehicle traffic, especially in cities, the number of pedestrian bridges has also increased significantly. Like all other structures, pedestrian bridges also suffer damage. In order to increase the safety of pedestrians, it is necessary to identify existing damage and to repair them to ensure the safety of the bridge structures. Owing to the shortcomings of local methods in identifying damage and in order to enhance the reliability of detection and identification of structural faults, signal methods have seen significant development in recent years. In this research, a new methodology, based on cone-shaped kernel distribution with a new damage index, has been used for damage detection in pedestrian truss bridges. To evaluate the proposed method, the numerical models of the Warren Type steel truss and the Arregar steel footbridge were used. Based on the results, the proposed method and damage index identified the damage and determined its location with a high degree of precision. Given the ease of use, the proposed method can be used to identify faults in pedestrian bridges.

Keywords: pedestrian truss bridges; damage detection; cone-shaped kernel distribution; time-frequency distribution

1. Introduction

The occurrence of failures in buildings, bridges, oil platforms and, in general, all structural systems during the life of the structure are inevitable. So far, samples of many types of faults have been recorded in different structures that resulted in considerable damage and mortality. Most of these structural failures can be corrected and repaired by initial evaluations of the existing state of the structures. This prevents the spread of structural damage and collapse of buildings. This is particularly true for earthquake-prone areas, where the local damage in structural elements can be the source of general damage (Walia *et al.* 2015, Mohammadi *et al.* 2016). Therefore, if damage detection becomes possible in structural elements, repair or replacement of damaged elements can prevent general damage to the structure. Thus, identification and damage detection systems can play a very important role in the immunization and repair of structures, and, thus, prevent financial and material losses caused by the collapse of structural systems (Pyayt *et al.* 2014, Seyedpoor *et al.* 2018). Structural damage can generally be caused by various factors such as poor construction, improper maintenance, overloading, and exposure to chemical agents such as sulfates, chloride ions, and atmospheric factors such as freezing and watering cycles such as earthquakes. Among these factors, earthquakes are the most destructive of all, and their destruction mechanism is somewhat

different from those of other factors, and since they can cause severe damage to a structure within a short time, special attention is needed with regard to them (Wenzel 2009, Zhou *et al.* 2015). Locally, methods for detecting damage such as ultrasonic, radiography, magnetic field and penetrating material are time-consuming, costly, and they sometimes face accessing difficulties (Kaloop *et al.* 2016, Cao *et al.* 2017). In order to overcome these disadvantages, general deterioration detection methods, based on the overall behavior of a structure, have been developed to determine the extent of damage and its location. Experiments that are performed in general methods to detect structural damage can be done using static or dynamic loading. In addition, some of the characteristics of the behavior of a structure can be measured, such as the displacement of certain points, the strain of the members, the frequency of the vibration modes, the shape of the vibration modes, and other behavioral characteristics. Then, based on the results, the presence of damage and its location and severity are determined (Ditomaso *et al.* 2015, Danna and Mekonnen 2012). Among the types of damage, cracks are one of the most important reasons for structural failures. The effect of cracking in a structure usually occurs in the form of changes in local stiffness. These changes have a significant effect on the dynamic characteristics of structures. This phenomenon is significant in changing the natural frequencies and mode shapes of structures, and an analysis of these changes makes it possible to detect cracks (Doebbling *et al.* 1996, Zhou 2008). In the signal techniques, changes in structural characteristics are obtained directly from the measured time history signals. The signal methods are divided into three categories: time-domain methods, frequency-domain methods, and time-frequency domain methods. In the methods of time and frequency domains,

*Corresponding author, Assistant Professor

E-mail: ahmadi@maragheh.ac.ir

^aM.Sc.

stationary and linear signals should usually be used (Bonato *et al.* 2000, Roy *et al.* 2012). For example, the AR model can be used for stationary signals, and if used to process non-stationary signals, self-movement parameters become difficult to estimate. The ARMA is often used to process stationary signals (Walia *et al.* 2015, De lautour 2008). The use of this method to process non-stationary signals increases the computational time. Additionally, the moving average autoregressive model satisfactorily processes only moderated signals with linear frequency and amplitude (Ahmadi *et al.* 2015). The basis of most of the frequency-domain methods such as frequency response functions (FRF) and spectral power density (SPD) are based on the Fourier transform (Neild *et al.* 2003, Melhem and Kim 2003). The Fourier transform is used to calculate the frequency contents of signals, but cannot determine the event time of the frequency components. In other words, the Fourier transform is suitable for the processing of signals whose frequency contents do not change with time. However, if the frequency contents of the signal changes with time, the Fourier transform cannot provide complete information about the behavior of the system (Powell and Allahabadi 1988, Abdul Awal and Boashash 2016). By using the Fourier transforms, the frequency contents of the signal is defined as a set of weighted sinusoid functions, but other important information such as the change in the signal's characteristics is not identified. Owing to these limitations, other methods have of late been suggested that process signals simultaneously in the time domain and the frequency domain (Dung 2013, Pnevmatikos *et al.* 2016, Pnevmatikos and Hatzigeorgiou 2017).

The basic principles of time-frequency functions have been long established, but, so far, the use of square time-frequency functions has been rarely reported in the extraction of the characteristic and the identification of the system and, in particular, the detection of damage in bridges (Yan *et al.* 2007, Ghiasi *et al.* 2016, O'Brien and Malekjafarian 2016). In this study, the use of square time-frequency functions is proposed to derive the dynamic characteristics of footbridge structures. Usually, structures in civil engineering have non-stationary responses and sometimes their responses are affected by nonlinear behavior. The advantage of the time-frequency functions is that they can process all signals including stationary, non-stationary and non-linear signals (Li and Ou 2016, Nikos *et al.* 2016, Pnevmatikos and Hatzigeorgiou 2017). Often, it is difficult to detect signal characteristics by viewing the time-domain graph, but the use of time-frequency functions adds another dimension to the signal diagram, and the frequency content is displayed with time and vice versa (Bradford 2006, Wang *et al.* 2018). A time-frequency function, by giving the frequency content with respect to time variations, provides the possibility of optimal signal analysis. Time-frequency functions are classified into linear, quadratic, and nonlinear types (Cohen 1989, Rucka 2011). Using the time-frequency analysis, it is possible to display the signal energy in the time and frequency domains simultaneously (Qiao 2009, Elhatab *et al.* 2016).

In this study, for the first time, a cone-shaped kernel distribution has been used for system identification and

damage detection in bridges. In this research, a new methodology has been proposed to identify damage caused to the deck of steel truss pedestrian bridges. Based on the proposed methodology, the bridge deck is vibrated with an exciting load before and after damage and its response signals are recorded. The registered signals are processed by cone-shaped kernel distribution and time-frequency plans, and matrices are calculated. The results are assessed with a new damage index. Finally, using the proposed methodology and damage index, faults and their locations are identified.

2. Cone-shaped kernel distribution

Time-frequency representations have extensively been used in the processing of signals in various fields. They express the variations of the frequency contents versus the signal time. A well-known form of the time–frequency representation introduced by Cohen (1966) is given below (Cantero and Basu 2015)

$$C_x(t, f; \pi) = \int_{-\infty}^{\infty} \int_{-\infty}^{\infty} \pi(s-t, \xi-f) W_x(s, \xi) ds d\xi \quad (1)$$

where $W_x(s, \xi)$ is the Wigner-Ville distribution of the signal $x(t)$ (Žibert *et al.* 2002). The Wigner-Ville distribution is the most prominent quadratic time-frequency representation. It has good mathematical properties and excellent time-frequency resolution, but it also produces substantial cross terms. Due to this important defect, other time-frequency representations have been proposed. It should be noted, most other TFR can be derived from the Wigner-Ville distribution, with a suitable choice of kernels. The alternative definition of Cohen's class representations can be interpreted as the 2D Fourier transform of the ambiguity function $A_x(\xi, \tau)$ which is multiplied by the kernel $k(\xi, \tau)$ as below

$$C_x(t, f; k) = \int_{-\infty}^{\infty} \int_{-\infty}^{\infty} K(\xi, \tau) A_x(\xi, \tau) e^{j2\pi(f\tau + \xi t)} d\xi d\tau \quad (2)$$

$A_x^*(\xi, \tau)$ is the complex conjugate of ambiguity function. If $K(\xi, \tau)=1$, the result is actually the Wigner-Ville distribution. If $A_x^*(\xi, \tau)$ is used as the $K(\xi, \tau)$ in Eq. (2) the spectrogram distribution would be created. The spectrogram is the square of the short-time Fourier transform and is defined as below

$$S_x(t, f) = \left| \int_{-\infty}^{\infty} x(u) h^*(u-t) e^{j2\pi fu} du \right|^2 \quad (3)$$

In order to suppress the cross terms from the basic distribution of the Cohen class, some improved distributions have been proposed. The cone-shaped kernel distribution (CKD) is one the best quadratic time–frequency representation for signal processing (Liu 2017). CKD keeps the specification of finite time support and can improve spectral peaks and reduce cross-terms (Peng and Weng 2008). On the other hand, CKD significantly improves the frequency resolution and provides improved cross-term

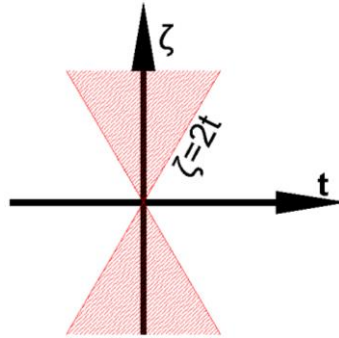


Fig. 1 The used support region of the cone-shaped kernel

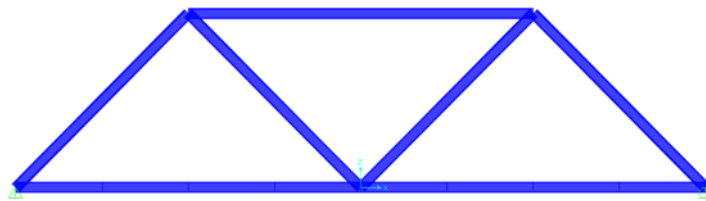


Fig. 2 View of the numerical model of Warren Type steel truss



Fig. 3 A side view of Arregar pedestrian bridge

suppression and higher resolution in the derived spectrum (Skeberis *et al.* 2015). In fact, CKD produces a good resolution in time and frequency domains, and reduces interference resulting from the cross-terms present in multi components signals (Urresty *et al.* 2009, Maheswari and Umamaheswari 2017). Therefore, in this research, CKD was used to process the signals. CKD is defined as (Žibert *et al.* 2002, Chen and Zhou 2007)

$$CKD_x(t, f) = \int_{-\infty}^{\infty} h(\tau) \left[\int_{t-|\tau|/2}^{t+|\tau|/2} x(s+\tau/2)x^*(s-\tau/2)ds \right] e^{j2\pi f\tau} d\tau \quad (4)$$

$h(\tau)$ is the smoothing window. To control the bandwidth of low pass filter, finite and smooth function, $h(\tau)$ is selected as the cone function, which is defined as

$$h(\tau) = \frac{1}{2} \exp(-\alpha\tau^2) \quad (5)$$

where α is the parameter that is used to adjust the cone slopes in the range of $2 \leq \alpha \leq \infty$. The used support region of the cone-shaped kernel is displayed in Fig. 1.

3. Bridge analytical models

To evaluate the performance of the methodology and proposed damage index, two different structures are considered. The first structure is Warren Type steel truss, and the second structure is a steel truss footbridge.

3.1 Warren type steel truss

A simple two-dimensional truss was used as the first model. The steel truss, shown in Fig. 2, is of the Warren Type and has 7 elements and 5 nodes. Warren Type trusses are widely used in many structures, including footbridges. The length of the truss was 24 meters and its height about 6 meters. The truss was modeled, and modal analysis results

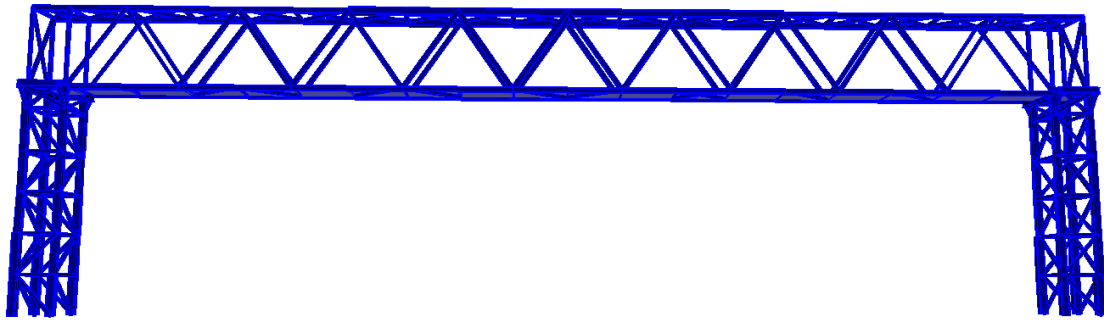


Fig. 4 3D view of the numerical model of Arregar steel truss pedestrian bridge

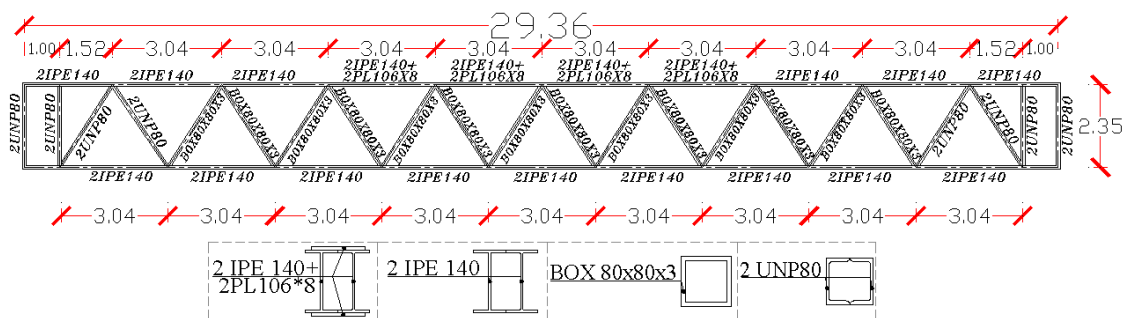


Fig. 5 The sections used in Arregar deck

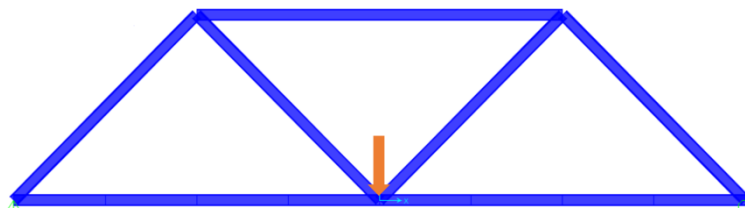


Fig. 6 Place of application of cosine stimulus load on the steel truss

were compared with Mehrjoo *et al.* (2008) for verification. As shown in Table 1, the natural frequencies of the first four modes of the model are similar to those of Mehrjoo *et al.* (2008).

3.2 Arregar steel truss footbridge

The second structure considered in this research was the Arregar steel truss footbridge. The Arregar pedestrian bridge is about 27.36 meters long and 2.1 meters wide.

Table 1 Comparison of natural frequencies of Analytical model for Warren Type truss

modal number	calculated natural frequency	natural frequency from Mehrjoo <i>et al.</i> (2008)
1	13.143 Hz	13.16 Hz
2	20.611 Hz	20.62 Hz
3	26.841 Hz	26.84 Hz
4	41.427 Hz	41.42 Hz

In addition, the height of the truss is 2.35 meters. The bridge is located in the Nezam Pezeshki street of Tabriz. The finite element model of the bridge is based on as-built details. Fig. 3 shows a side view of the bridge. Its numerical model can be found in Fig. 4. In addition, the sections used in the bridge deck are displayed in Fig. 5. During the construction, the steel used in the bridge was tested in 2015. The average yielding stress, and the average ultimate stress of steel samples have been calculated, and the results were used to update the model. The results are shown in Table 2. Furthermore, after the completion of the bridge, its condition has been assessed and the finite element model evaluated by in situ measurements.

4. Bridge analytical models

The assessment of the safety of pedestrian bridges and their serviceability is of great importance. Considering the importance of the subject, this research proposes a new approach to distinguish faults in pedestrian bridges. The

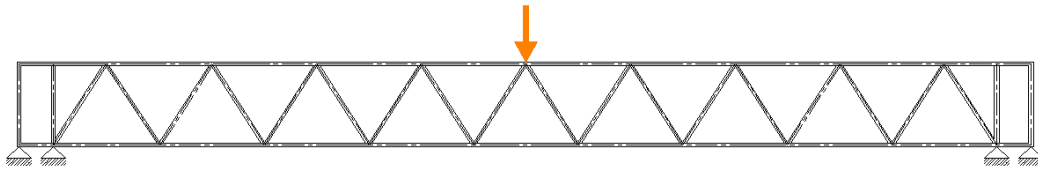


Fig. 7 Place of application of cosine stimulus load on the footbridge

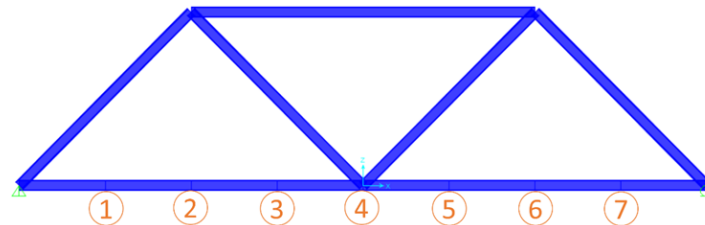


Fig. 8 Sensor places at Warren Type truss

proposed approach is designed to be easy to use for pedestrian bridges and to identify damage. Based on the approach, a force with a specific frequency and low amplitude was applied to the bridge deck at the middle of the length. In this study, a cosine force with an angular frequency equal to π was used to excite the models. In fact, the angular frequency of the excitation load is different with the dominant frequencies of the structures. The excitation load considered in this research is chosen to be applicable to pedestrian bridges. The amplitude of the load is considered equal to 50 N, which can be easily produced by exciters (Bien and Zwolski 2008). The duration of the excitation force was 5 seconds. The deck response was recorded on some of the deck's nodes. In other words, it was assumed that the accelerometer sensors were mounted at some nodes of the bridge deck, and the vibrations of the bridge were recorded. This process was performed before and after the faults occurred on the pedestrian bridge. Owing to the faults, the vibrations of the bridge changed. These changes near the damage locations were greater than the other structural regions. This is the main idea considered in the proposed algorithm. The proposed algorithm is designed in such a way that it can specify the changes in bridge vibration. The proposed algorithm involves the use of CKD to identify the system and the new damage index to detect faults in the steel-truss footbridge.

5. Confirmation of the proposed algorithm and damage index

5.1 Model not damaged

Based on the methodology, a harmonic cosine load was applied to the models and its responses were registered after a time history analysis. The excitation force was applied in the middle of the span of the structures. Figs. 6 and 7 show the loading location on the steel truss and the bridge deck respectively.

Table 2 Test results of the strength of materials used in Arregar steel truss footbridge

row	Material	Yielding stress of steel (MPa)	Ultimate stress of steel (MPa)
1	steel	237	354

Seven sensors, shown in Fig. 8, were considered in the Warren Type steel truss to record the vibration of the truss. In addition, at the deck level of the footbridge, 8 points were considered as the sensor locations in order to measure the structure response. These points were the same in all damage scenarios. In Fig. 9, the location of the sensors is shown on the deck surface of the footbridge. Besides, the coordinates of sensor locations are displayed in Table 3.

Table 3 Coordinates of sensor locations

Sensor number	X(m)
1	3
2	6
3	9
4	12
5	15
6	18
7	21
Arregar steel truss pedestrian bridge	
Sensor number	X(m)
1	4.04
2	7.08
3	10.12
4	13.16
5	16.20
6	19.24
7	22.28
8	25.32

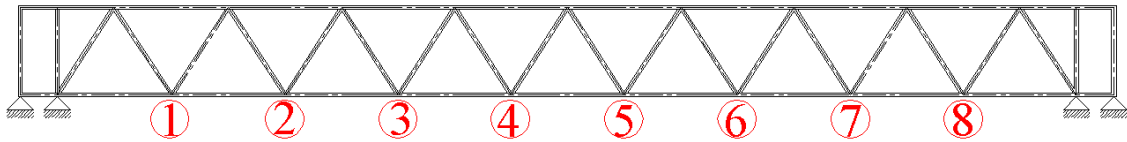


Fig. 9 Location of sensors in Arregar steel truss pedestrian bridge

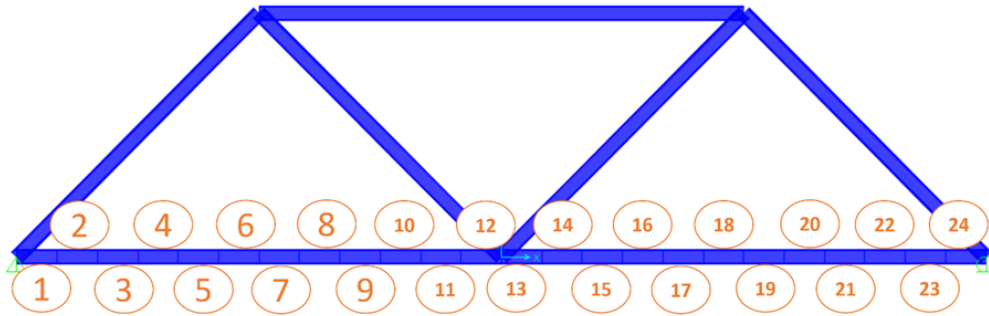


Fig. 10 The simple truss element numbers

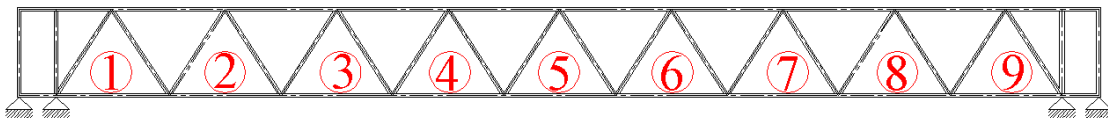


Fig. 11 The footbridge element numbers

5.2 Damaged model

In order to investigate the damage detection method for the steel truss and the pedestrian bridge, four and six different damage scenarios were considered respectively. These failures were considered by reducing by 15%, 30%, and 50% the sectional thickness in the numerical models. The damage scenarios are presented in Tables 4 and 5.

Table 4 The damage scenarios for Warren Type truss

scenario	Damaged element	Damage(%)
1-T	5	15%
2-T	5	30%
3-T	5	50%
4-T	3 - 22	50%

Table 5 The damage scenarios for the footbridge

Damage(%)	Damaged element	scenario
15%	4	1-P
30%	4	2-P
50%	4	3-P
15%-50%	5-9	4-P
30%-30%	5-9	5-P
50%-50%	5-9	6-P

Besides, the element numbers for Warren Type truss and Arregar steel truss footbridge are shown in Figs. 10 and 11 respectively. Regarding the length of 12 meters of truss bottom chord members, each one is divided into 12 elements of one meter. As seen in Table 4, in damage scenario 4-T, damage is considered simultaneously in two different elements. Based on Table 5, in damage scenarios 4-P to 6-P, faults of different intensities in two elements were applied simultaneously.

6. Processing of recorded signals from footbridge

As stated, the response signals of the structures were recorded under the influence of cosine loading before and after the damage. The cone-shaped kernel distribution, which is a square time-frequency representation, was used to process Warren Type truss and Arregar steel truss footbridge signals.

7. Methodology used and method of doing research

7.1 Suggested damage index (Θ index)

A new damage index is proposed in the research to diagnose damage in the truss footbridge. The time-frequency matrices, calculated by the cone-shaped kernel distribution, were used. H and F are the symbol of Healthy

matrix and Faulty matrix respectively. On the other hand, H represents the time-frequency matrix of the undamaged structure and F indicates the time-frequency matrix of the damaged structure. The matrix form generated by the cone-shaped kernel distribution is shown in Fig. 12. The subscript h indicates the healthy state that is rewritten as f in the damaged condition.

The formulas and mathematical relationships used to calculate the suggested damage index are as follows

$$\pi_{Hi} = \sum_{j=1}^n H(v_i, \tau_j) = \begin{bmatrix} CS\hat{K}_h(v_m) \\ CS\hat{K}_h(v_{m-1}) \\ \vdots \\ CS\hat{K}_h(v_1) \end{bmatrix} \quad (6)$$

$$\mu_{Hi} = \begin{bmatrix} \frac{CS\hat{K}_h(v_m)}{n} \\ CS\hat{K}_h(v_{m-1}) \\ \vdots \\ \frac{CS\hat{K}_h(v_1)}{n} \end{bmatrix} \quad (7)$$

$$\tilde{H} = \begin{bmatrix} CSK_h(v_m, \tau_1) - \mu_{H_m} \\ CSK_h(v_{m-1}, \tau_1) - \mu_{H_{m-1}} \\ \vdots \\ CSK_h(v_1, \tau_1) - \mu_{H_1} \\ CSK_h(v_m, \tau_2) - \mu_{H_m} \quad \dots \\ CSK_h(v_{m-1}, \tau_2) - \mu_{H_{m-1}} \quad \dots \\ \vdots \quad \dots \\ CSK_h(v_1, \tau_2) - \mu_{H_1} \quad \dots \\ CSK_h(v_m, \tau_n) - \mu_{H_m} \\ CSK_h(v_{m-1}, \tau_n) - \mu_{H_{m-1}} \\ \vdots \\ CSK_h(v_1, \tau_n) - \mu_{H_1} \end{bmatrix} \quad (8)$$

$$\Pi_{\tilde{H}i} = \sum_{j=1}^n \tilde{H}(v_i, \tau_j) = \begin{bmatrix} CS\tilde{K}_h(v_m) \\ CS\tilde{K}_h(v_{m-1}) \\ \vdots \\ CS\tilde{K}_h(v_1) \end{bmatrix} \quad (9)$$

Similar calculations are made for the F matrix. Finally, the following matrix is obtained

$$\Pi_{\tilde{F}i} = \sum_{j=1}^n \tilde{F}(v_i, \tau_j) = \begin{bmatrix} CS\tilde{K}_f(v_m) \\ CS\tilde{K}_f(v_{m-1}) \\ \vdots \\ CS\tilde{K}_f(v_1) \end{bmatrix} \quad (10)$$

The proposed damage index is described below

$$\Theta = \Pi_{\tilde{H}i}^T \otimes \Pi_{\tilde{F}i} \quad (11)$$

Using Θ index, the damage and its location is determined. As mentioned, the dimensions of the time-frequency matrices are proportional to the steps of recording the response signals. In this research, the registration frequency of the response signal is equal to 100Hz. In addition, in order to increase the resolution of time-frequency plans, the number of time and frequency bins equal to the number of steps is considered. However, the dimensions of the time-frequency matrices in this study are 950 to 950, given that Warren Type truss and the footbridge have 3 and 8 sensors respectively. Therefore, the number of Θ index for each scenario in the Warren Type truss is equal to 3 and in pedestrian bridge it is equal to 8. However, in each of the damage scenarios in the simple truss, 3 numbers are calculated as Θ_1, Θ_2 and Θ_3 . In addition, 8 values including Θ_1, Θ_2 to Θ_8 are calculated in the pedestrian bridge. If the values of Θ indices are zero, they indicate that no damage has occurred in the beam. Otherwise, it would mean the occurrence of damage. In this case, the indices are normalized, based on a larger index. Then, a comparison of the results leads to the detection of the damage. A larger value certainly indicates the location of the damage.

7.2 Calculated results

The calculation of the results done on the basis of the proposed algorithm is shown in the Figs. 13 to 22:

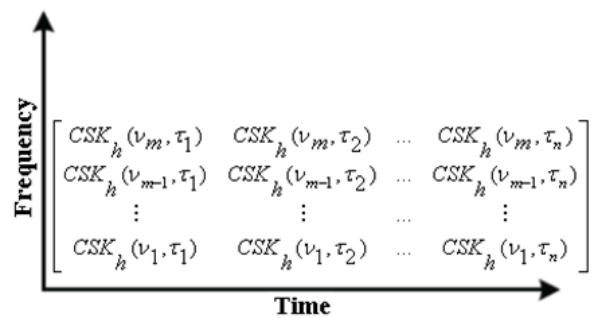


Fig. 12 The matrix form of cone-shaped kernel distribution

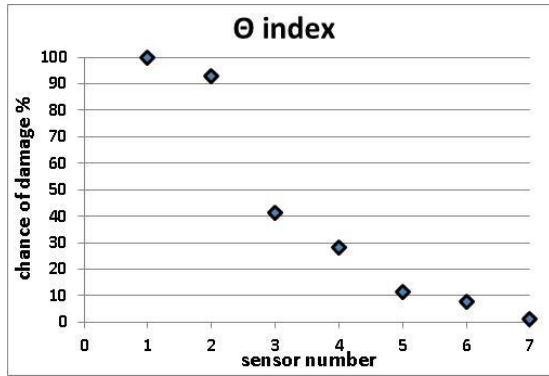


Fig. 13 Diagnostic Diagram of damage for Scenario 1-T

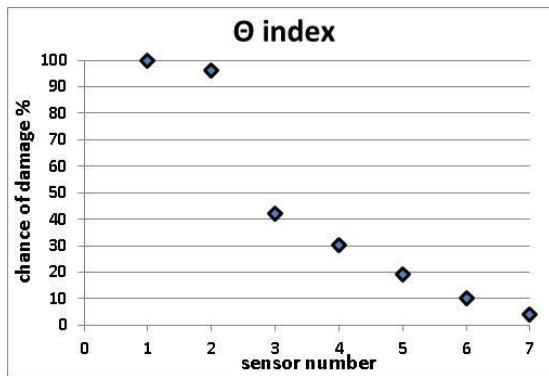


Fig. 14 Diagnostic Diagram of damage for Scenario 2-T

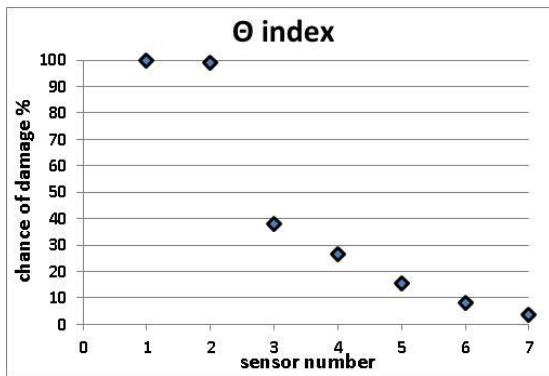


Fig. 15 Diagnostic Diagram of damage for Scenario 3-T

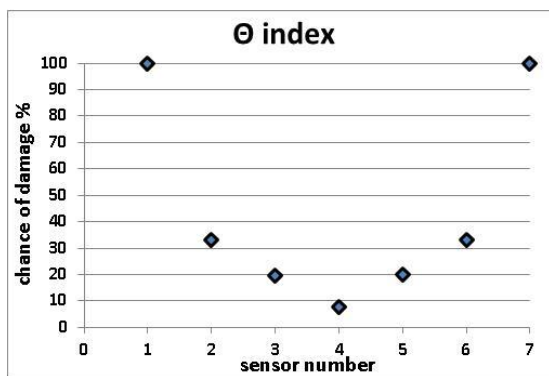


Fig. 16 Diagnostic Diagram of damage for Scenario 4-T

7.2.1 Calculated results for Warren Type steel truss

The obtained using proposed methodology and Θ index for Warren Type steel truss were shown in this subsection. Considering Figs. 13-16, it can be seen that the unhealthy element has been correctly distinguished by using Θ index. In scenario 1-T, the damage is considered in element 5. In fact, the damage is considered in a small element, which is difficult to identify because of the long length of the member and the small number of sensors. Sensors 1 and 2 are located on the sides of element 5. As shown in Fig. 13, despite the low severity and length of the damage, element 5 is signally identified as the damaged element using Θ index. Regarding Table 4, in scenarios 2-T and 3-T, the damage is considered in element 5 with greater intensity. In Figs. 14 and 15, it is seen that the proposed index correctly diagnoses the damaged element. In addition, with an increasing severity of damage, the unhealthy element is more accurately identified by Θ index. In scenario 4-T, damage is considered simultaneously in elements 3 and 22. The damage was likely to be detected at the location of sensor 1 and 7, if Θ index were to correctly identify the damaged elements. Based on the calculations shown in Fig. 16, the use of the proposed methodology and damage index identified elements 5 and 24 as unhealthy. Although the damage was considered in small elements and two elements were damaged simultaneously, Θ index correctly and accurately identified the faults.

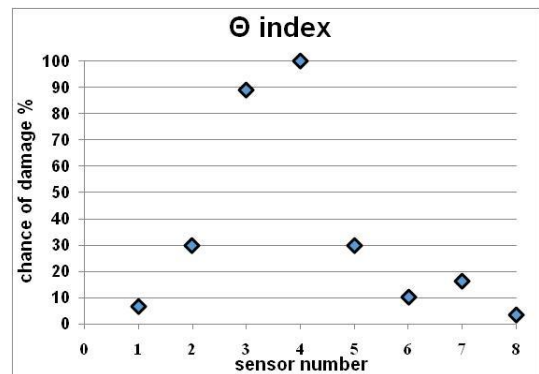


Fig. 17 Diagnostic Diagram of damage for Scenario 1-P

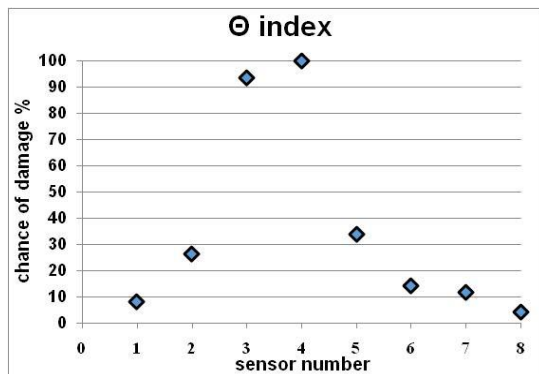


Fig. 18 Diagnostic Diagram of damage for Scenario 2-P

7.2.2 Calculated results for Arregar steel truss footbridge

The results obtained for Arregar steel truss footbridge are shown in Figs. 17-22. Based on the results, the algorithm and suggested damage index identified the affected location in the pedestrian truss bridge correctly. In scenarios 1-P, 2-P and 3-P, the damage with different intensity is considered in element 4. As shown in Figs. 9 and 11, sensors 3 and 4 are located on the sides of the element 4. However, damage was likely to be detected at the location of sensors 3 and 4, if Θ index were to correctly diagnose the faults. In other words, Θ index was to show results nearly 100% in the locations of sensors 3 and 4.

It can be seen in Figs. 17-19 that the damage was accurately detected at the location of sensors 3 and 4. Scenarios 4-P, 5-P, and 6-P, too, which simultaneously caused two faults, the algorithm could correctly detect them. Elements 5 and 9 were damaged due to various intensities in the scenarios. Element 5 is located between sensors 4 and 5 and element 9 is located between sensor 8 and right bearing. According to Table 5, in scenario 4, the damage extents considered simultaneously in elements 5 and 9 are equal to 15% and 50% respectively. This scenario is a difficult test to evaluate the performance of the suggested damage index. After the calculation, in location of sensor 9, the value of Θ index was equal to 100%. Besides, the magnitude of the damage index in sensors 4 and 5 was significantly higher than in sensors 1, 2, 3, 6 and 7. However, despite the two faults of varying intensities, Θ index correctly identified them and their locations.

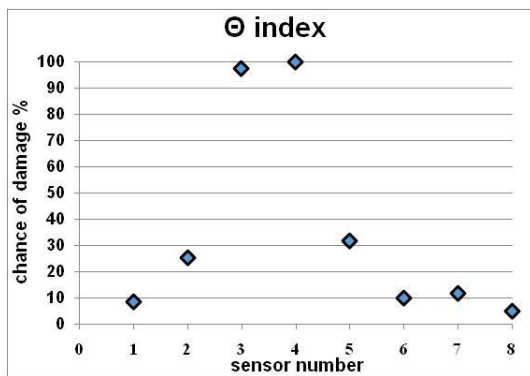


Fig. 19 Diagnostic Diagram of damage for Scenario 3-P

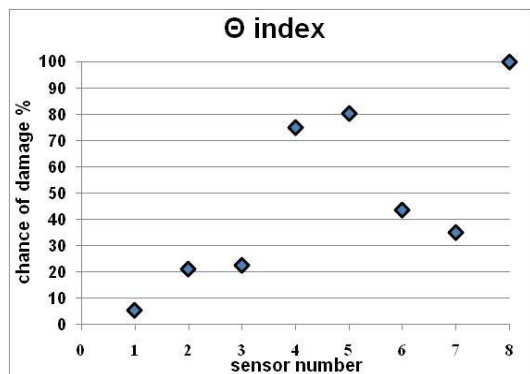


Fig. 20 Diagnostic Diagram of damage for Scenario 4-P

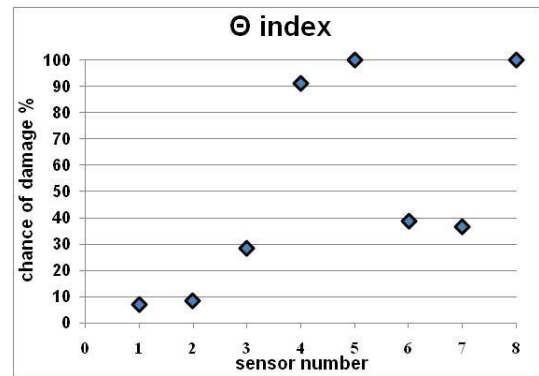


Fig. 21 Diagnostic Diagram of damage for Scenario 5-P

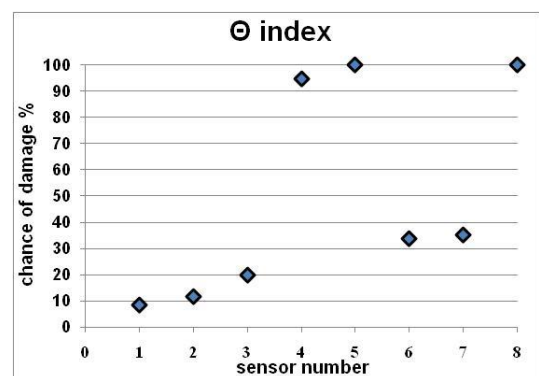


Fig. 22 Diagnostic Diagram of damage for Scenario 6-P

In scenarios 5-P and 6-P, damage is considered simultaneously in elements 5 and 9. As shown in Table 5, the damage in scenarios 5-P and 6-P are assumed to be equal to 30% and 50% respectively. Figs. 21 and 22 show that the damaged elements have been accurately detected at the locations of sensors 4 and 5, as well as 9.

Therefore, it is apparent from the results that the proposed algorithm and damage index show a very good performance in detecting damage and identifying its location.

8. Conclusions

There are many pedestrian bridges around the world. Some of these bridges have been damaged due various reasons such as a relatively high lifetime, corrosion, fatigue and so on. Considering the number of footbridges, it is important to have methods that can easily and quickly detect damage with high precision. This research, for the first time, presents the application of a cone-shaped kernel distribution for detecting damage and identifying its location in a steel pedestrian bridge. As shown, the proposed algorithm is constructed in such a way that it is not necessary to construct a bridge analytical model. Based on the existing experience in structural health monitoring, the algorithm is output-only and does not require the measurement of input loading. Another feature of the

proposed algorithm is its ability to simultaneously identify damage at several points. The performance of the new methodology and proposed damage index was evaluated on Warren Type steel truss and Arregar steel truss pedestrian bridge. For this purpose, different damage scenarios were defined. Based on the calculated results and using the methodology and Θ index, the defined damage was detected and its location accurately determined. In addition, if some elements are simultaneously damaged, the proposed algorithm and index are able to detect the damaged elements with high precision. Therefore, due to the simplicity of the proposed algorithm and the features and characteristics of the proposed method, it can be used for monitoring the health of steel pedestrian bridges.

Acknowledgments

The authors are extremely grateful of the support given by GRAF(Group of Arman Faraz Pol) Consulting Engineers Co. and are particularly appreciative.

References

- Abdul Awal, M.D. and Boashash, B. (2016), "Time-frequency image enhancement based on interference suppression in Wigner-Ville distribution", *Signal Process.*, **127**, 80-85.
- Ahmadi, H.R., Daneshjoo, F. and Khaji, N. (2015), "New damage indices and algorithm based on square time-frequency distribution for damage detection in concrete piers of railroad bridges", *Struct. Control Health Monit.*, **22**(1), 91-106.
- Bien, J. and Zwolski, J. (2007), "Dynamic tests in bridge monitoring-systematics and applications", *Proceedings of the IMAC-XXV: conference & exposition on structural dynamics*, 1-10, Orlando.
- Bonato, P., Ceravolo, R., De Stefano, A. and Molinari, F. (2000), "Use of cross-time-frequency estimators for structural identification in non-stationary conditions and under unknown excitation", *J. Sound Vib.*, **237**(5), 779-791.
- Bradford, S. (2006), "Time-frequency analysis of systems with changing dynamic properties", PhD thesis, California Institute of Technology, USA.
- Cantero D. and Basu B. (2015), "Railway infrastructure damage detection using wavelet transformed acceleration response of traversing vehicle", *Struct. Control Health Monit.*, **22**(1), 62-70.
- Cao, M.S., Sha, G.G., Gao, Y.F. and Ostachowicz, W. (2017), "Structural damage identification using damping: a compendium of uses and features", *Smart Mater. Struct.*, **26**(4), 043001.
- Chang, C.M. and Huang, S.K. (2016), Matrix factorization to time-frequency distribution for structural health monitoring. In *Sensors and Smart Structures Technologies for Civil, Mechanical, and Aerospace Systems*, **9803**, 98031S.
- Chen, G.X. and Zhou, Z.R. (2007), "Time-frequency analysis of friction-induced vibration under reciprocating sliding conditions", *Wear*, **262**(1-2), 1-10.
- Cohen, L. (1989), "Time-frequency distributions-a review", *Proceedings of the IEEE*, **77**(7), 941-981.
- Danna, N.M. and Mekonnen, E.G. (2012), "Data Processing Algorithms in Wireless Sensor Networks for Structural Health Monitoring", Master of Science Thesis, Royal Institute of Technology (KTH), Stockholm, Sweden.
- De laoutour O.R. (2008), "Assessment of seismic damage to civil structures using statistical pattern recognition techniques and time series analysis", PhD thesis, University of Auckland, New Zealand.
- Ditommaso, R., Ponzo, F.C. and Auletta, G. (2015), "Damage detection on framed structures: modal curvature evaluation using Stockwell transform under seismic excitation", *Earthq. Eng. Eng. Vib.*, **14**(2), 265-274.
- Doebbling, S.W., Farrar, C.R., Prime, M.B. and Shevitz, D.W. (1996), "Damage identification and health monitoring of structural and mechanical systems from changes in their vibration characteristics: A Literature Review", Los Alamos National Laboratory, LA-13070-Ms, USA.
- Dung, H. (2013), "Damage detection in structures using Frequency Response Function (FRF) data and finite element modeling", Master thesis, Victoria University of Technology, Melbourne, Australia.
- Elhatab, A., Uddin, N. and O'Brien, E. (2016), "Drive-by bridge damage monitoring using bridge displacement profile difference", *J. Civil Struct. Health Monit.*, **6**(5), 1-12.
- Ghiasi, R., Torkzadeh, P. and Noori, M.A. (2016), "machine-learning approach for structural damage detection using least square support vector machine based on a new combinational kernel function", *Struct. Health Monit.*, **15**(3), 302-316.
- Kalooop, M.R., Hu, J.W. and Elbeltagi, E. (2016), "Time-series and frequency-spectrum correlation analysis of bridge performance based on a real-time strain monitoring system", *ISPRS International Journal of Geo-Information*, **5**(5), 61.
- Li H. and Ou, J. (2016), "The state of the art in structural health monitoring of cable-stayed bridges", *J. Civil Struct. Health Monit.*, **6**(1), 43-67.
- Liu, Z. (2017), "Detection and estimation research of high-speed railway catenary", Springer Nature Singapore Pte Ltd, Singapore.
- Maheswari, R.U. and Umamaheswari, R. (2017), "Trends in non-stationary signal processing techniques applied to vibration analysis of wind turbine drive train-A contemporary survey", *Mech. Syst. Signal Pr.*, **85**, 296-311.
- Mehrojoo, M., Khaji, N., Moharrami, H. and Bahreininejad, A. (2008), "Damage detection of truss bridge joints using Artificial Neural Networks", *Exp. Syst. Appl.*, **35**(3), 1122-1131.
- Melhem, H. and Kim, H. (2003), "Damage detection in concrete by Fourier and Wavelets analysis", *J. Eng. Mech.*, **129**(5), 571-577.
- Mohammadi, M., Pouyan, A.A. and Khan, N.A. (2016), "A highly adaptive directional time-frequency distribution", *Signal, Image Video Process.*, **10**(7), 1369-1376.
- Neild, S.A., McFadden, P.D. and Williams, M.S. (2003), "A review of time-frequency methods of structural vibration analysis", *Eng. Struct.*, **25**, 713-728.
- O'Brien, E.J. and Malekjafarian, A. (2016), "A mode shape-based damage detection approach using laser measurement from a vehicle crossing a simply supported bridge", *Struct. Control Health Monit.*, **23**(10), 1273-1286.
- Peng, Y. and Weng, X. (2008), "IFMBE Proceedings", Beijing, China.
- Pnevmatikos, N.G., Blachowski, B., Hatzigeorgiou, G.D., and Swiercz, A. (2016), "Wavelet analysis based damage localization in steel frames with bolted connections", *Smart Struct. Syst.*, **18**(6), 1189-1202.
- Pnevmatikos, N.G. and Hatzigeorgiou, G.D. (2017), "Damage detection of framed structures subjected to earthquake excitation using discrete wavelet analysis", *Bull. Earthq. Eng.*, **15**(1), 227-248.
- Powell, G.H. and Allahabadi, R. (1988), "Seismic damage prediction by deterministic methods; concepts and procedures", *Earthq. Eng. Struct. D.*, **28**, 79-104.
- Pyayt, A.L., Kozionov, A.P., Mokhov, I.I., Lang, B., Meijer, R.J.,

- Krzhizhanovskaya, V. and Sloot, P.M.A. (2014), "Time-frequency methods for structural health monitoring", *Sensors*, **14**(3), 5147-5173.
- Qiao, L. (2009), "Structural damage detection using signal-based pattern recognition", PhD thesis, Kansas State University, USA.
- Roy, K., Ogai, H., Bhattacharya, B., Ray-Chaudhuri, S. and Qin, J. (2012), "Damage detection of bridge using wireless sensors", *IFAC Proceedings Volumes*, **45**(23), 107-111.
- Rucka, M. (2011), "Damage detection in beams using wavelet transform on higher vibration modes", *J. Theor. Appl. Mech.*, **49**(2), 399-417.
- Seyedpoor, S.M., Norouzi, E. and Ghasemi, S. (2018), "Structural damage detection using a multi-stage improved differential evolution algorithm (Numerical and experimental)", *Smart Struct. Syst.*, **21**(2), 235-248.
- Skeberis, C., Zaharis, Z.D., Xenos, T.D., Spatalas, S., Arabelos, D. N. and Contadakis, M.E. (2015), "Time-frequency analysis of VLF for seismic-ionospheric precursor detection: Evaluation of Zhao-Atlas-Marks and Hilbert-Huang Transforms", *Phys. Chem. Earth, Parts A/B/C*, **85**, 174-184.
- Walia, S.K., Patel, R.K. and Vinayak, H.K. (2015), "Time-frequency and wavelet-based study of an old steel truss bridge before and after retrofitting", *J. Civil Struct. Health Monit.*, **5**(4), 353-363.
- Wenzel, H. (2009), "Health monitoring of bridges", John Wiley & Sons Ltd, West Sussex, UK.
- Wang, Z., Qiao, P. and Shi, B. (2018), "Effective time-frequency characterization of Lamb wave dispersion in plate-like structures with non-reflecting boundaries", *Smart Struct. Syst.*, **21**(2), 195-205.
- Yan, Y., Cheng, L., Wu, Z. and Yam, L. (2007), "Development in vibration-based structural damage detection technique", *Mech. Syst. Signal Pr.*, **21**, 2198-2211.
- Žibert, J., Mihelič, F. and Pavešić, N. (2002), "Speech features extraction using cone-shaped kernel distribution", *Proceedings of the International Conference on Text, Speech and Dialogue*, 245-252, Springer, Berlin, Heidelberg.
- Zhou, X., Xia, Y. and Weng, S.H. (2015), "L₁ regularization approach to structural damage detection using frequency data", *Struct. Health Monit.*, **14**(6), 571-582.
- Zhou, Z. (2008), "Vibration-based damage detection of simple bridge superstructures", PhD thesis, University of Saskatchewan, Canada.
- Urresty, J., Riba, J., Ortega, J. and Cárdenas, J. (2009), "Stator short circuits detection in PMSM by means of Zhao-Atlas-Marks distribution and energy calculation", *Proceedings of the 13th European Conference on Power Electronics and Applications*, 1-9, IEEE.